Paper 04211

Symposium on
AC corrosion Mechanisms and Control

AC-INDUCED CORROSION IN PIPELINES:
DETECTION, CHARACTERISATION, AND MITIGATION

L.V. Nielsen and K.V. Nielsen
MetriCorr ApS, info@metricorr.dk
Glerupvej 20, DK-2610 Roedovre, Denmark

B. Baumgarten
HNG I/S – Greater Copenhagen Natural Gas
Gladsaxe Ringvej 11, DK-2860 Soeborg, Denmark

H. Breuning-Madsen
Institute of Geography, University of Copenhagen
Oester Voldgade 10, DK-1350 Copenhagen K

P. Cohn
DONG National Oil and Gas Company of Denmark
Agern Allé 24-26, 2970 Hoersholm, Denmark

H. Rosenberg
Balslev Consulting Engineers A/S
Produktionsvej 2, DK-2600 Glostrup, Denmark

ABSTRACT

By connecting AC corrosivity probes to AC interfered pipelines the accumulated as well as instant corrosion rate can be assessed. Simultaneously adjusting and monitoring of the electrical (AC/DC) conditions of the pipeline, the corrosion rate can be measured as a function of these parameters. Measurements performed in the field confirm a mechanism of AC induced corrosion which involves local alkalization of the local soil environment close to a coating defect. An intelligent switch devise (ISD) has been presented which controls earthing of the pipeline via capacitors. When a timer is connected to the CP rectifier in connection with CP surveys (ON/OFF potential measurements) the ISD detects the regularly pulsed (ON/OFF) CP and disconnects the earthing system thus allowing for instant OFF measurements of the CP potential. In combination with the AC corrosivity probes, a concept is provided similar to management of internal corrosion by controlled inhibitor dosage carefully adjusted and optimized by use of on-line and real time intrusive corrosivity probes.

Keywords: AC corrosivity probe, on line - real time monitoring, AC corrosion mechanisms, corrosion rate vs. AC voltage, AC mitigation by intelligent switch device.

INTRODUCTION

Buried pipelines provided with high resistance coatings are susceptible to induction of AC voltage from paralleling high-voltage AC power lines. This AC-voltage may be a cause of corrosion at coating defects where the AC current escapes the pipe. The electrical equivalent diagram of a pipeline with superimposed AC may be sketched as in figure 1[1]. The electrochemical conditions as well as the CP rectifier produce electromotive forces. $E_0 1$ and $E_0 2$ denote equilibrium potentials relating to those electrochemical processes that are active at a coating defect (e.g. ferrous corrosion and hydrogen production). VB1 and VB2 are components analogous to diodes and represent (Volmer-Butler) activation kinetics of involved processes. Warburg impedance component (W) is coupled to indicate influence of diffusion limitation. R_S (also known as spread resistance) denotes the ohmic resistance from pipe to remote earth, and C denotes interfacial capacitance. The AC generator refers to AC on pipe due to induction from a paralleling high-voltage power line. Such induction can be correlated with the magnitude of current transmitted in the adjacent parallel power line. Figure 2 illustrates an example from the Danish gas grid system. The level of the transmitted AC current varies on a daily basis and magnitude of the induced AC voltage on the pipe changes accordingly (in figure 2 between 1 and 10 V – 50 Hz in the Danish system).

It is believed[2-5] that one mechanism of AC induced corrosion involves alkalisation of the local environment around a coating defect due to enhanced cathode kinetics etc, which in combination with induced AC creates corrosive conditions. It has been shown that both AC induced passivity breakdown at moderately high pH values can occur, as well as high pH general corrosion[2-5]. The dashed lines in the Pourbaix-diagram (figure 3) illustrate the critical potential-pH domain. Small rather than large coating defects are susceptible to AC corrosion since the spread resistance (in $\Omega.m^2$) associated with the defects increases with increasing area[1]:

$$R_s = K \cdot \rho_s \cdot d \quad (\Omega.m^2) \tag{1}$$

where K is a constant depending on the geometry of the defect, d is a measure of the extension of the defect, and ρ_s is the specific resistivity of the local soil environment adjacent to the defect. To build up a critical local high pH soil environment, the spread resistance has to be very low (0.1 $\Omega.m^2$ or less), which maintains a high level of current flowing through the defect. In practice this eliminates AC corrosion to occur in environments rich in earth alkaline cations (Ca^{2+}, Mg^{2+}) since these form cathodic scaling products which increases (by several orders of magnitude) the spread resistance[2].

This paper illustrates how AC induced corrosion can be quantified and monitored in the field using highly sensitive AC corrosivity probes connected to the pipeline which can measure the instantaneous corrosion rate. Results reflect the mechanisms described above. An intelligent switch device (ISD) is described and qualified which mitigates AC by draining the AC current using earth electrodes coupled to the pipe via bipolar capacitors. By combining usage of AC corrosivity probes and AC mitigation by ISD, a concept is provided similiar to minimizing internal corrosion by controlled inhibitor dosage carefully adjusted and optimized by use of on-line and real time intrusive corrosivity probes.

EXPERIMENTAL PROCEDURES

ER Based AC Corrosivity Probe

The AC corrosivity probe with associated instrumentation is based on the high-resolution differential electrical resistance concept presented previously[6,7]. The technique utilizes the fact that the electrical resistance of a metal probe element increases when corrosion diminishes the thickness of the element. Referring to simple plate geometry for a metal element with dimensions L (length), W (width), and σ (thickness), the electrical resistance of the element can be expressed by:

$$R = \rho\,(T) \cdot \frac{L}{W \cdot \sigma} \tag{2}$$

where $\rho(T)$ is the specific resistivity of the element material.

Re-arranging equation (2) gives the thickness of element expressed as a function of element resistance:

$$\sigma = \rho\,(T) \cdot \frac{L}{W} \cdot \frac{1}{R} \tag{3}$$

Differentiation of this equation gives the corrosion rate V_{corr} of the element as:

$$V_{corr} = -\frac{d\sigma}{dt} = \frac{dR}{dt} \cdot \frac{W}{L} \cdot \frac{\sigma^2}{\rho(T)} \tag{4}$$

Hence, if positioned in a corrosive environment, knowledge of the time change of the electrical resistance of the element, the element dimensions, and resistivity of the element material, the corrosion rate can be quantified. It follows by re-arranging equation (4) that the period of time needed to quantify a certain corrosion rate can be assessed by:

$$\Delta t = \frac{\Delta R}{V_{corr}} \cdot \frac{W}{L} \cdot \frac{\sigma^2}{\rho(T)} \tag{5}$$

The equation predicts that the necessary period of time increase with increasing W/L ratio, and increases with the square of the element thickness. Hence, high sensitivity ER probes can be produced by using thin elements, but this decreases probe lifetime as well. In equation (5), ΔR can be regarded as the minimum resistance change needed to provide a reliable measurement. Improvement of the resolution of the applied ohm-meter then allows for shortening of the necessary period of time needed to quantify a certain corrosion rate without compromising in terms of probe element lifetime. In the present concept, a resolution in the region of 0.1 $\mu\Omega$ is realized through improved differential instrumentation[6,7]. The ER based AC corrosivity probe is shown in figure 4. The active area of the simulated coating defect is typically 0.4 cm^2. Both real-time high-resolution corrosion rate measurements and traditional element thickness measurements can be performed on the probes.

Field Stations for AC Corrosivity Monitoring.

The AC corrosivity sensors are installed in standard measuring posts and connected to the pipe. Traditional ER technique is used to monitor whether changes of the element thickness occurs over time, and in such case the high-resolution measurement can be applied for real time monitoring of the corrosion rate while CP and grounding procedures are optimized. The principle of a field measuring circuitry is shown in figure 5. The probes are connected via 10 ohm resistors across which the AC and DC current can be quantified. Optionally a variable resistor has been inserted for easy adjustment of the magnitude of the AC voltage experienced by the probe. This resistor is positioned in series with the spread resistance of the probe, the sum of which is conducting the level of AC current flowing through the probe. By proper adjustment of this resistor, the AC level on the probe can be adjusted. This procedure is applicable since the spread resistance is orders of magnitude lower than the polarization resistance of the electrochemical system which essentially governs the DC characteristics. In one case referred to here (HNG site), the series resistor was replaced with a bipolar capacitor which eliminated the rectifier current and allowed only the AC part to flow through the probe.

In this paper, 2 research programs are referred to. One campaign has been conducted on a field station owned by DONG – the National Oil- and Gas Company of Denmark, and a second campaign has been conducted on a station owned by HNG – Greater Copenhagen Natural Gas. Results from theses stations have been picked out among several other locations where traditional ER measurements have shown non-corrosive conditions due to formation of high spread resistances (1-10 $\Omega.m^2$) on the probes. The main purpose of the campaigns was to establish the corrosion rate as a function of the AC voltage thus being able to define levels below which no corrosion occurs.

AC Mitigation by an Intelligent Switch Device Installed in Standard Measuring Posts

For the purpose of decreasing AC voltages below the above defined acceptable limits, earthing of the pipeline is required through electric capacitors (bipolar, electrolytic), which is a reliable and affordable measure to prevent AC-corrosion. It is a safe approach that does not jeopardize the cathodic protection.
Verification of cathodic protection requires that the capacitors can be disconnected from the pipeline for CP-survey measurements. Important CP-data on AC-influenced pipelines can however only be collected during low to moderate AC-influence periods. Often such periods are relatively limited and short, and they may appear on inconvenient hours. For this reason, an Intelligent Switch Device (ISD) has been designed and manufactured which automatically disconnects the capacitors from the pipeline when a regularly pulsating ON/OFF-potential is sensed by the microprocessor incorporated in the ISD – see figure 6. A pipeline operator saves man-hours when collecting cathodic protection data from the pipelines without manually having to disconnect the capacitors. Additionally, the ISD maintains the required safety against hazardous touch voltages in all operation modes. Installed in the measuring post, the ISD is connected to the pipeline and a local earth electrode. A bipolar electrolytic capacitor is installed together with the ISD. When the AC-voltage, experienced by the ISD, exceeds 3.5 volt the ISD "wakes up" and a pipe to earth connection via the capacitor will be established. The ISD remains in this (active) mode until either of the following two things happens:

1. The alternating current through the ISD becomes less than 180 mA.
2. The DC-potential is shifting regularly between "ON" and "OFF".

The first parameter ensures that the AC-mitigation is maintained even at very low influence levels. It also provides a hysteresis that prevents oscillating between active and inactive mode. The second parameter controls the interruption of the capacitor, when required. The ISD which is powered by the AC voltage from the pipe returns to active mode when/if the AC-voltage exceeds 3.5 volt and the DC-potential is stable.

The earth electrodes will not only mitigate electromagnetic induced AC-voltages under normal operation conditions, but also the much higher AC-voltages that can appear in case of an earth fault on the influencing high voltage line. The ISD is capable of handling 900 A for up to 0.2 second. Large currents (50/60 Hz) are conducted directly to the earth electrode, bypassing the electrolytic capacitor. The same applies to lightning induced surges, appearing on the pipeline. This is not only a measure to secure safe operation of the pipeline; it also provides an important protection for the electrolytic capacitor.

Location of earth electrodes along an AC-influenced pipeline is based on a calculation of the AC-voltage on the pipeline under normal/maximum operation load on the influencing high voltage lines. The electrode-resistance to remote earth must have realistic/obtainable values and the number should be as limited as possible.

RESULTS AND DISCUSSION

AC Corrosivity Monitoring at the DONG Site

Figure 7 shows the performance of the AC corrosivity probes when corroding moderately at the open circuit potential (OCP). In figure 7a, the increase in element resistance is plotted over a period of 10 hours illustrating the high-resolution of the device. In figure 7b, the resistance increase has been converted to elements thickness. Clearly, the slope of this curve can be calculated on a per hour basis, allowing for a real time monitoring of the corrosion rate.

Figure 8 shows – over a period of 3 weeks – the corrosion rate as well as the measured AC voltage (4-25V) on the pipe. By selecting a number of positions on these curves, the corrosion rate as a function of the voltage can be assessed (figure 9). This procedure leads to two stages of the corrosion process. In the initial stage, the corrosion rate seems to obey the equation:

$$V_{corr} = 0.45 \cdot e^{0.39 \cdot U_{AC}} \tag{6}$$

where V_{corr} is the corrosion rate in µm/yr) and U_{AC} is the AC voltage. In the steady state, the corrosion rate can be fitted into

$$V_{corr} = 0.85 \cdot e^{0.15 \cdot U_{AC}} \tag{7}$$

This behavior was taken as an indication of the mechanisms of AC corrosion. When connected to the pipeline, the local environment becomes alkalized and in combination with the oscillation of the potential caused by the induced AC, a destabilization of the passivating oxide layer is realized causing the corrosion. At zero AC the corrosion rate is zero. At continuous alkalization, the pH of the local environment becomes very high and the electrochemical conditions facilitate high-pH general corrosion.

AC Corrosivity Monitoring at the HNG Site

Figure 10 shows examples of spread resistance measurements and average corrosion rates for five different HNG test stations. Spread resistance varies over 3-4 decades and the corrosion rate seems to increase in general with decreasing spread resistance. It is noted that all of these stations have approximately the same level of AC induction on the pipe. Figure 11 shows results from the ER spot measurements of the element thickness at HNG station 3 ("Ølstykke" in figure 10). As observed, the connection of the probe to the cathodically protected pipe (112 days) certainly does not provide protection from corrosion, and the AC voltage initiates a corrosion process.

Figures 12 and 13 illustrate the results from the intensified campaign where – so far – 7 stages has been investigated. In stage 1, the probe was connected directly to the pipe. The ON-potential was here around -1400 mV CSE and AC variation between 1 and 12 V (figure 12). Quite high corrosion rates are obtained (up to 2 mm/y at 10 VAC). The spread resistance was measured against a large electrode placed in remote earth by a Saturn Geo earth tester, and in this case around 800 Ω or 0.03 $\Omega.m^2$ was obtained. Hence, the insertion of a series resistor of 800 Ω in stage 2 of the campaign reduced the AC experienced by the probe by around 50% (figure 12). The ON-potential was raised around 100 mV. The corrosion eventually stops in this stage (figure 13). In stage 3, the series resistor was adjusted to 2000Ω and corrosion died totally. In stage (4), the series resistor was replaced by a 5 mF bipolar capacitor. The interesting observation here is that the ON-potential increased to around 0 mV CSE and no corrosion occurs. In stage (5) the probe was disconnected from the pipe and allowed to corrode freely. After a period, the potential decreases and corrosion sets in on the probe. In stage (6) the probe was again connected directly to the pipe, and the ON potential re-establishes at -1400 mV and the probe corrodes according to the AC – however, not quite as high rates as in stage (1). In order to study the effect of the DC (ON) potential, the rectifier was adjusted in stage (7) so that the ON-potential rises to -850 mV CSE. The corrosion here tends to die out; however, this campaign is at present still on-going and further stages with different ON-potentials will be investigated.

In figure 14, the possible paths for the electrochemical conditions experienced by the probe have been sketched in the Pourbaix diagram. In stage (1) the cathodic protection current causes an alkalization of the local environment and corrosion sets in due to the high pH region in the diagram. The stages (2) and (3) with reduced AC as well as reduced DC causes a slight acidification process. Stage (4) raises the DC potential electropositively into the passive region, but probably with continuous acidification. During stage (5) at OCP conditions the acidification further progresses and the probe enters the general corrosion region of the diagram. Stage (6) reproduces stage (1) and stage (7) and proceeding stages where the ON potential is changed directly by the rectifier are still on-going, the question being if a proper adjustment of the DC potential can be used as well to control or reduce AC induced corrosion.

AC Mitigation by the ISD

Figure 15 shows AC voltage and DC potentials recorded throughout a 30-minute period at two points ("27836" and "24300") of a pipeline. A sequence is realized where:

1. The ISD's are in engaged mode (off-potentials can not be determined)
2. A timer/interrupter is activated in the CP station after 15 minutes,
3. The ISD's are deactivated automatically due to the ON/OFF pattern of the CP.

AC voltage is increasing stepwise as the capacitors along the pipeline are disconnected. Experience shows that it lasts from a couple of minutes up to one hour before all capacitors are disconnected from a pipeline. The capacitors are providing an attenuation of the "ON/OFF-signal". Therefore ISD's located nearest to the interrupting CP-station will disconnect their capacitors first, and the process will propagate along the pipeline until all capacitors are disconnected. From figure 15 is observed in the present context that the earthing procedures clearly reduce the AC voltage to levels which from the data presented in figures dramatically reduces the AC corrosion process and may in combination with the AC corrosivity sensors mounted along the pipe provide a system for management of AC induction with respect to the effect on corrosion risk.

CONCLUSIONS

Concepts of on-line real time AC corrosivity probes have been illustrated. By connecting such ER based probes to the AC interfered pipeline, the corrosion can be monitored both by periodic thickness measurements of the probe elements and as real time corrosion rate. By simultaneously adjusting and monitoring of the electrical (AC/DC) conditions of the pipeline, the corrosion rate can be measured as a function of these parameters. Measurements performed in the field confirm a mechanism of AC induced corrosion which involves local alkalization of the local soil environment close to a coating defect.

An intelligent switch devise (ISD) has been presented which controls earthing of the pipeline via capacitors. When a timer is connected to the CP rectifier in connection with CP surveys (ON/OFF potential measurements) the ISD detects the regularly pulsed (ON/OFF) CP and disconnects the earthing system thus allowing for instant OFF measurements of the CP potential. In combination with the AC corrosivity probes, a concept is provided similar to management of internal corrosion by controlled inhibitor dosage carefully adjusted and optimized by use of on-line and real time intrusive corrosivity probes.

REFERENCES

1. P. Cohn and L.V. Nielsen, AC corrosion and electrical equivalent diagrams. Proc. 5th international congress CeoCor, Brussels, Belgium, CeoCor, 2000.
2. F. Stalder et al., AC corrosion on cathodically protected pipelines, Proc. 5th international congress CeoCor, Brussels, Belgium, CeoCor, 2000.
3. A. Pourbaix et al, Proc. Eurocorr 2001, paper 228, Riva del Garda, Italy, EFC, 2001
4. L.V. Nielsen, Proc. Eurocorr 2001, paper 20, Riva del Garda, Italy, EFC, 2001.
5. L.V. Nielsen, Proc. 15th International Corrosion Congress, paper 796, Granada, Spain, ICC, 2002
6. International patent application, PCT/DK00/00689.
7. L.V.Nielsen, K.V.Nielsen, Differential ER-technology for measuring degree of accumulated corrosion as well as instant corrosion rate, CORROSION ´2003, Paper No. 03443, 2003
8. H. Rosenberg, AC mitigation with intelligent switch devices, Proc. CeoCor 2003
9. US Patent Application 10/172,098.

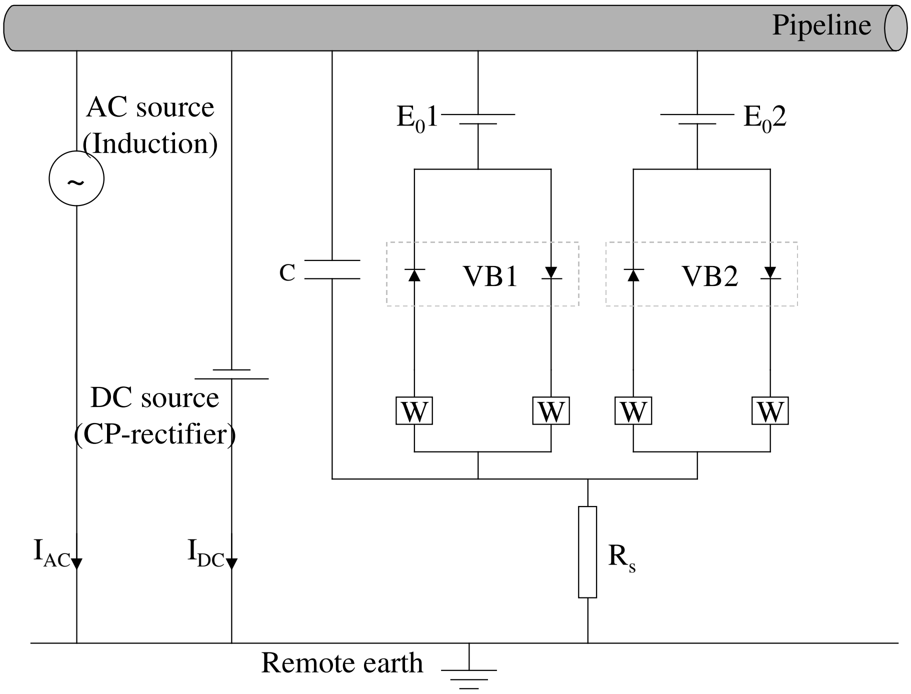

FIGURE 1 – Electrical equivalent circuit for AC interfered pipeline.

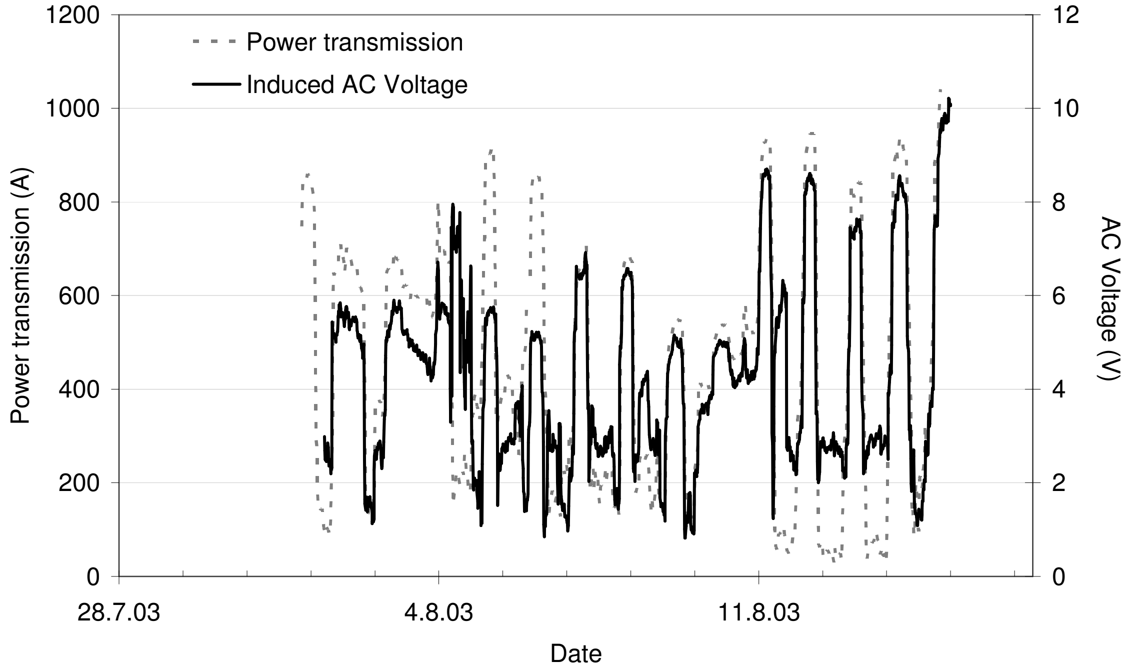

FIGURE 2 - Induced AC voltage compared with transmission current in paralleling high-voltage power line.

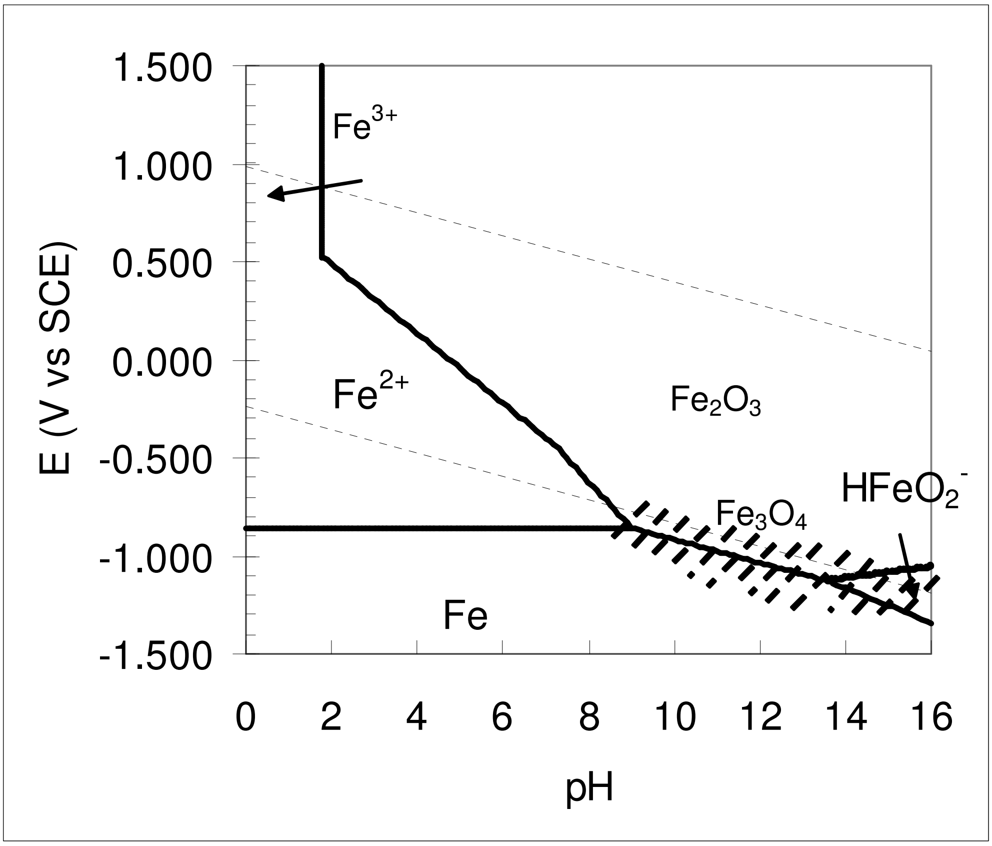

FIGURE 3 - Pourbaix-diagram showing area of AC induced passivity breakdown and area of high-pH general corrosion.

FIGURE 4 – AC corrosivity probe based on modified high-resolution ER principles.

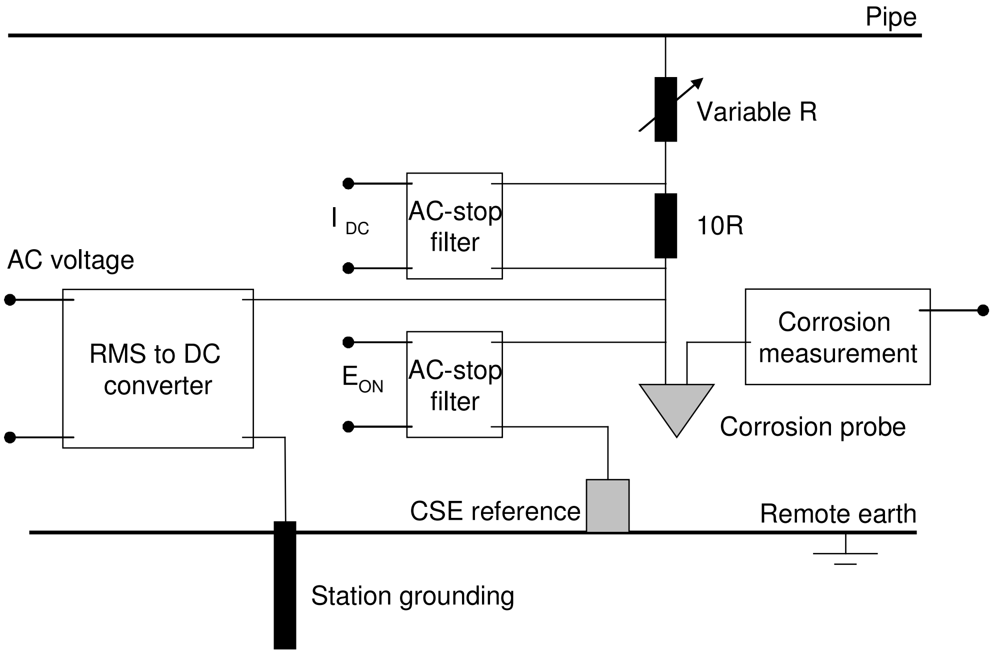

FIGURE 5 – Principles of field measurement circuit.

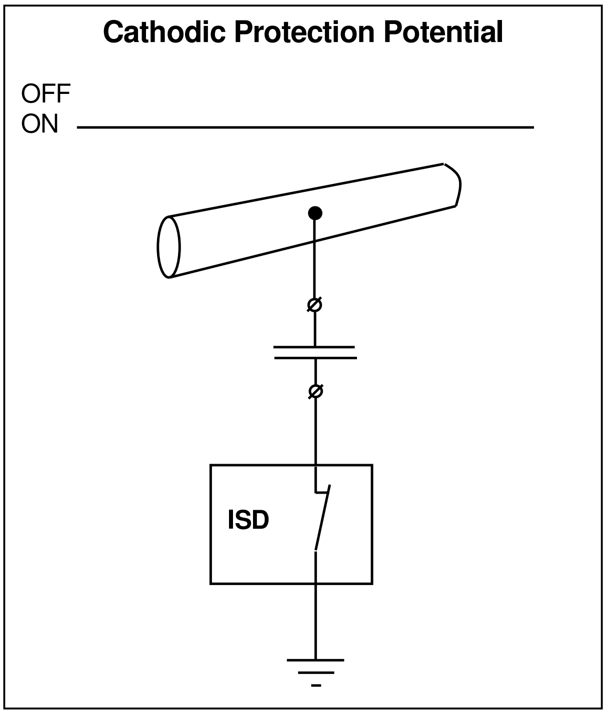

FIGURE 6a – At steady ON-potential the ISD drains the AC current through a capacitor.

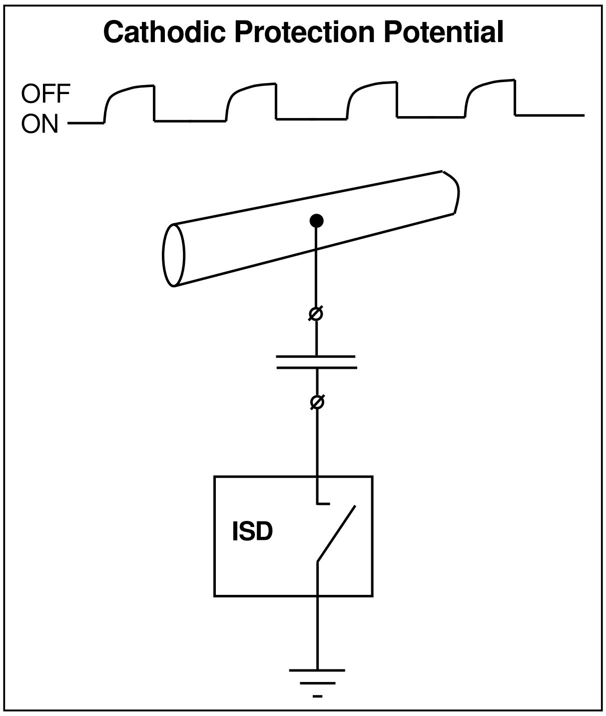

FIGURE 6b – At regularly pulsating ON/OFF potential, the ISD disconnects the capacitor.

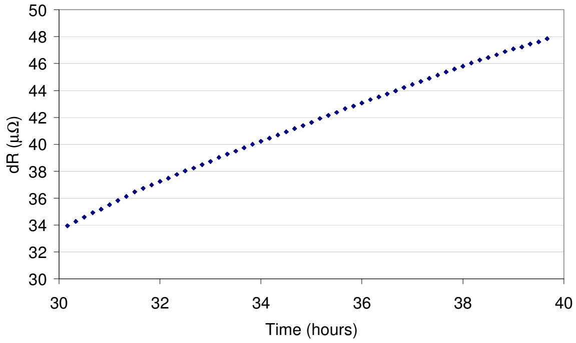

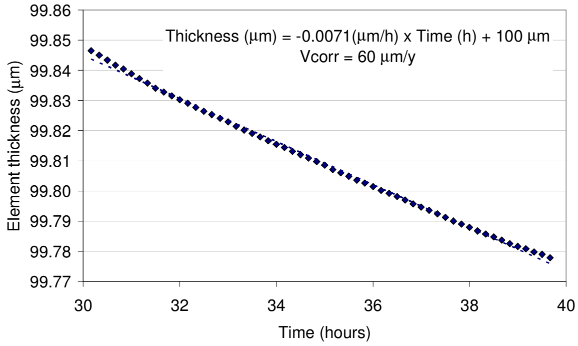

FIGURE 7a – Increase in element resistance during open circuit conditions.

FIGURE 7b – Response from ER measurement converted to element thickness.

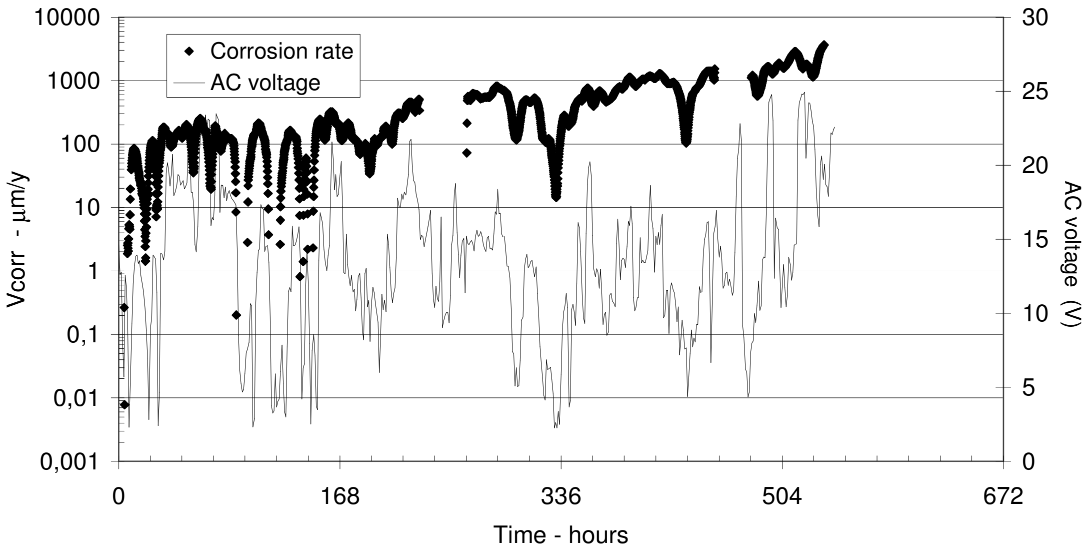

FIGURE 8 – Corrosion rate and AC voltage throughout time – DONG site.

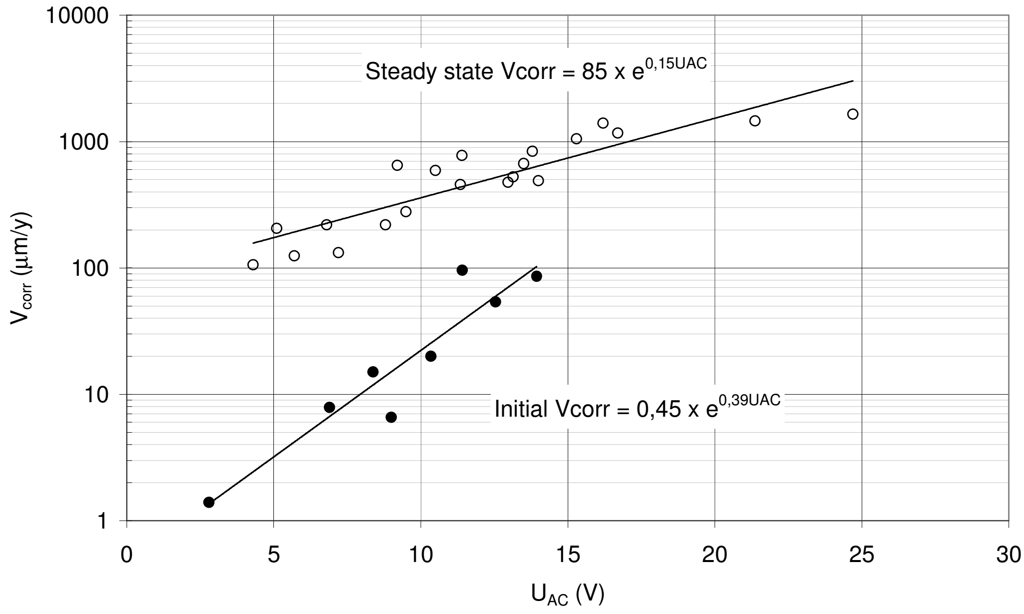

FIGURE 9 – Corrosion rate as a function of the AC voltage DONG site.

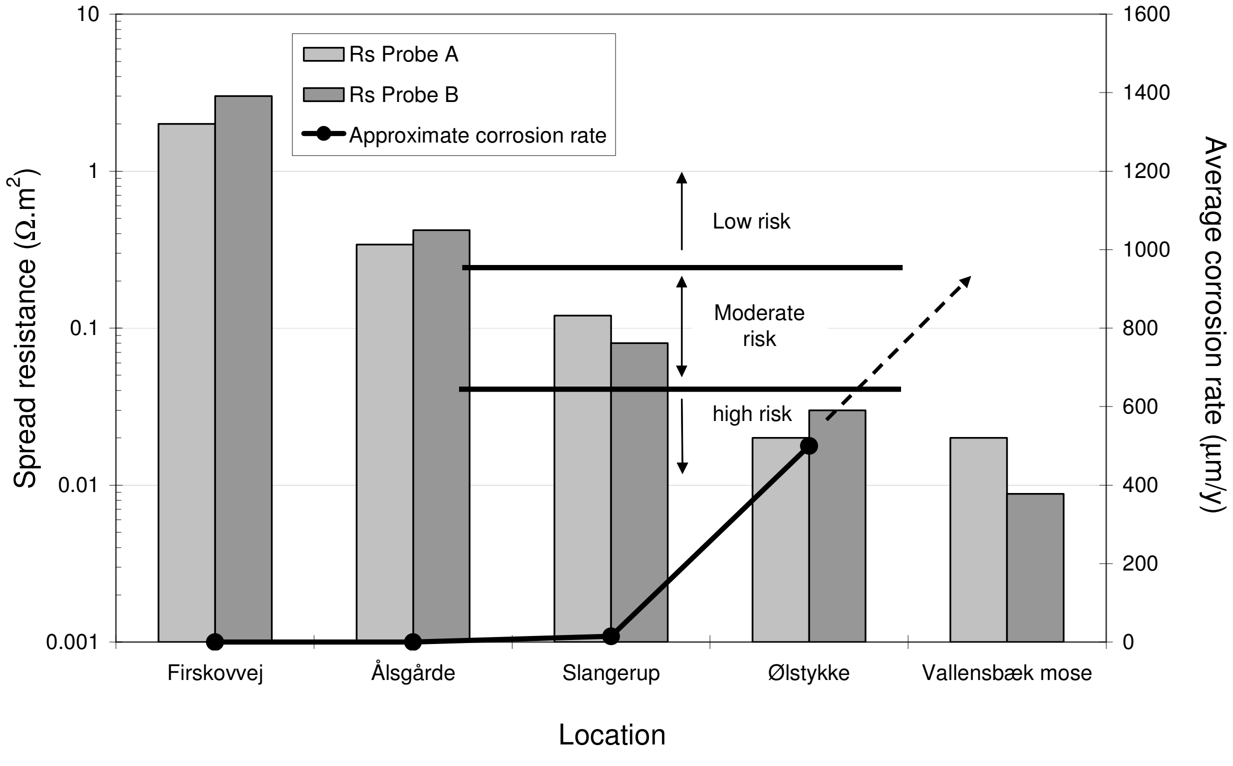

FIGURE 10 – Spread resistance measurements and corrosion rates determined by traditional ER thickness measurements at five different HNG sites.

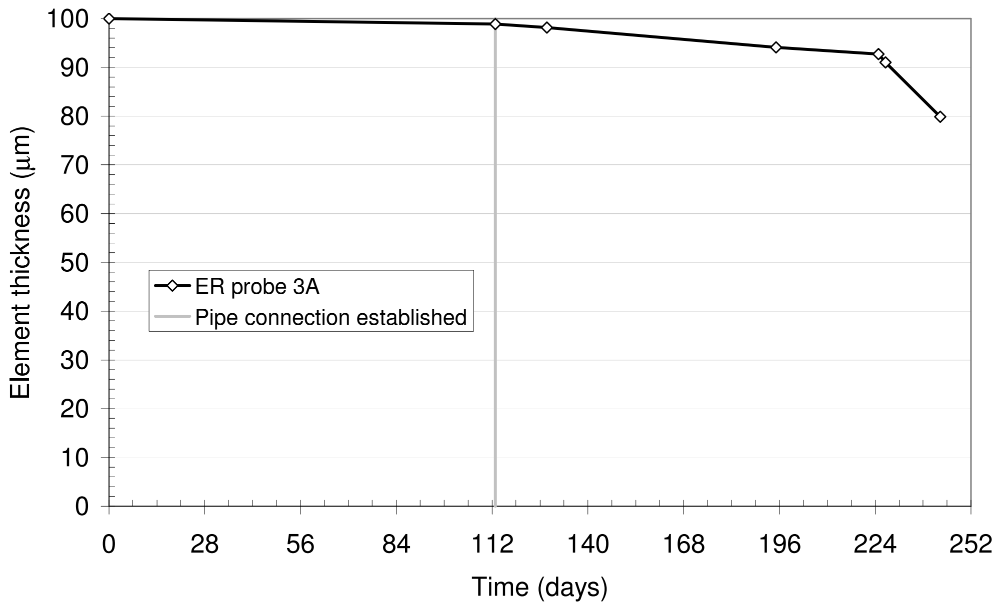

FIGURE 11 – Traditional ER spot measurements indicating corrosion after pipe connection (CP + AC) established on the probe – HNG site.

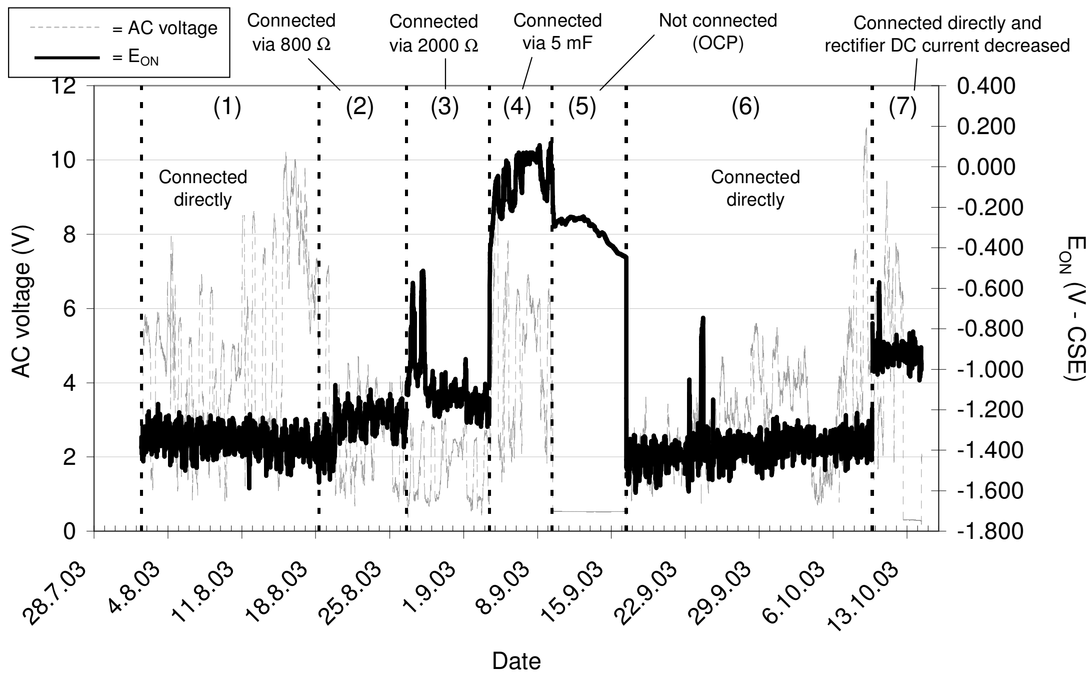

FIGURE 12 – AC voltage and ON-potential throughout time - HNG site.

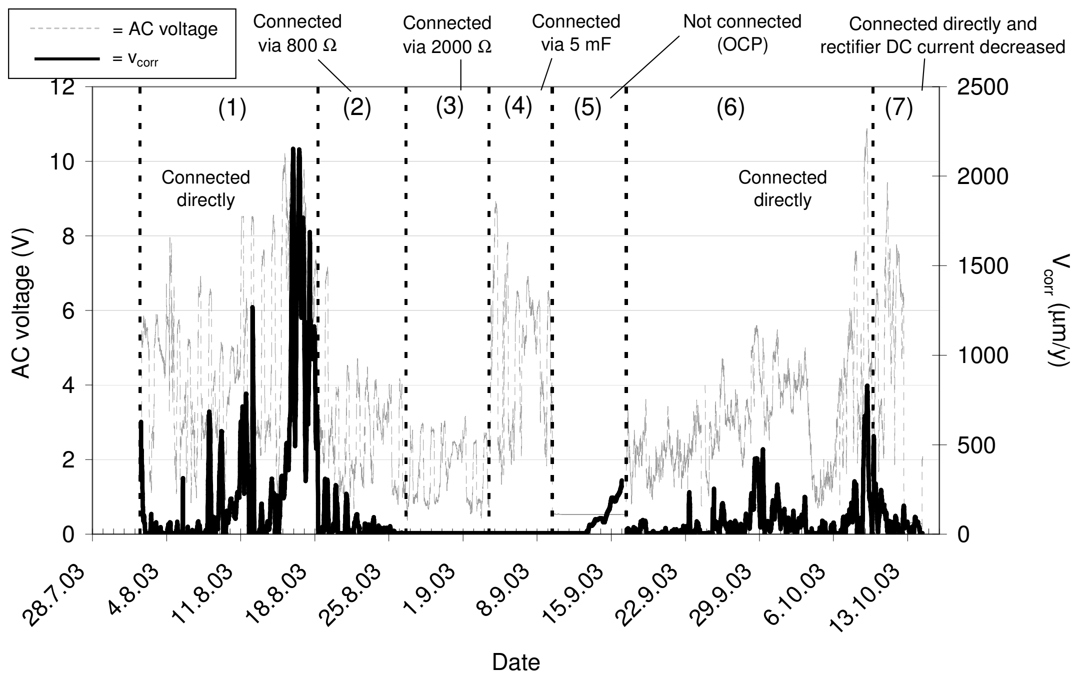

FIGURE 13 – AC voltage and corrosion rate - HNG site.

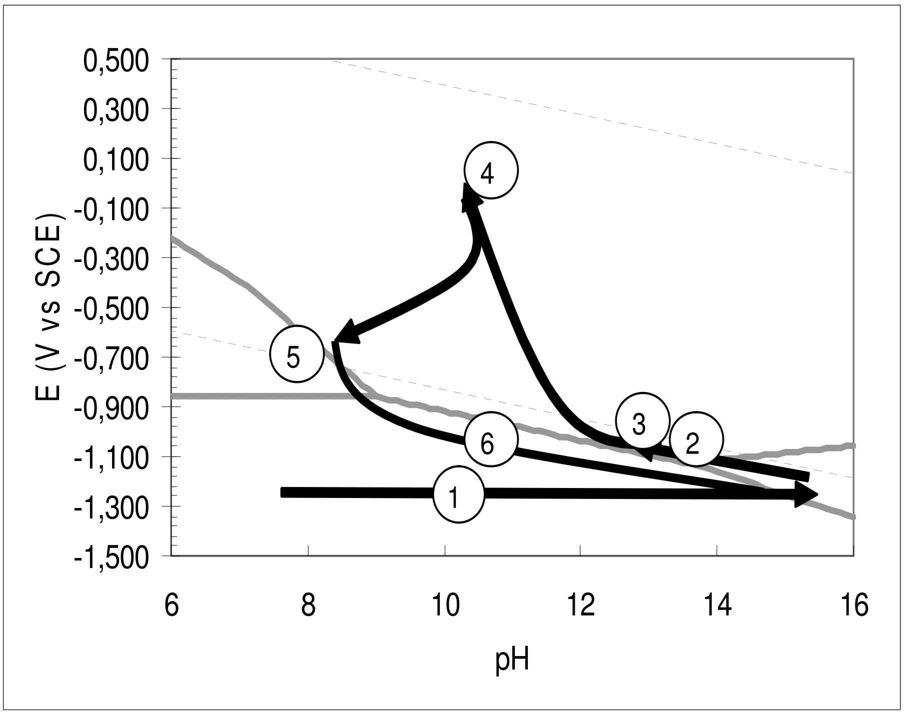

FIGURE 14 – Probable changes of probe conditions – HNG site.

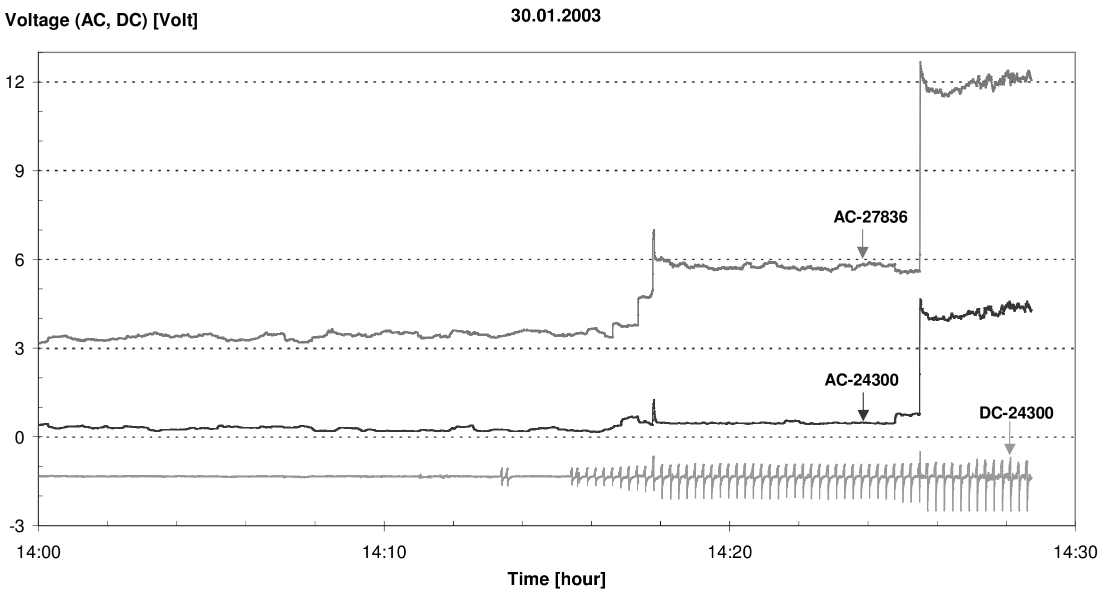

FIGURE 15 – Performance of the ISD when initiating regularly pulsed ON/OFF potential .

Figure captions:

FIGURE 1 – Electrical equivalent circuit for AC interfered pipeline.

FIGURE 2 - induced AC voltage compared with transmission level in paralleled high-voltage power line

FIGURE 3 - Pourbaix-diagram showing area of AC induced passivity breakdown and area of high-pH general corrosion.

FIGURE 4 – AC corrosivity probe based on modified high-resolution ER principles.

FIGURE 5 – Principles of field measurement circuit.

FIGURE 6a – At steady ON-potential the ISD drains the AC current through a capacitor.

FIGURE 6b – At regularly pulsating ON/OFF potential, the ISD disconnects the capacitor.

FIGURE 7a – Increase in element resistance during open circuit conditions.

FIGURE 7b – Response from ER measurement converted to element thickness.

FIGURE 8 – Corrosion rate and AC voltage throughout time – DONG site.

FIGURE 9 – Corrosion rate as a function of the AC voltage DONG site.

FIGURE 10 – Spread resistance measurements and corrosion rates determined by traditional ER thickness measurements at five different HNG sites

FIGURE 11 – Traditional ER spot measurements indicating corrosion after pipe connection (CP + AC) established on the probe – HNG site.

FIGURE 12 – AC voltage and ON-potential throughout time - HNG site.

FIGURE 13 – AC voltage and corrosion rate - HNG site.

FIGURE 14 – Probable changes of probe conditions – HNG site.

FIGURE 15 – Performance of the ISD when initiating regularly pulsed ON/OFF potential .